

the atactic isomer. Both these factors decrease the film thickness at which oxidation becomes diffusion controlled.

As diffusion of oxygen into the film is the rate-controlling step and if it is assumed that a type of Bolland mechanism⁸ is operative, then the initial stages of the oxidation process can be accounted for quantitatively. This will be demonstrated in part II of this paper. The amount of tertiary hydrogen atoms in the film and the initial oxygen pressure can be considered approximately constant for the initial stage of the oxidation reaction. The later stages of this process, however, become too complicated to be explained quantitatively; at best a semiquantitative account can be given and trends can be indicated. Volatiles produced by chain scission alone will consist only of quite small amounts during the initial stages. The volatiles formed during this initial stage must be almost exclu-

sively due to decomposition of hydroperoxide groups, which does not lead to chain scission. Actually, the main volatile product during the initial stage appears to be water.

As the oxidation proceeds beyond its initial stage, the oxygen pressure in the gas phase, the film thickness, and the medium viscosity decrease continuously; the latter decrease is due to chain scission. It may even be the case that eventually the chemical reaction will become rate determining.

Acknowledgment. The authors wish to thank the U. S. Army Office of Research, Durham, N. C., for a Grant No. DA-ARO-D-31-124-G984, which made this work possible. Thanks are also due to Dr. S. H. Ronel for carrying out experiments with polymer films of different thickness (see Figure 5).

Diffusion-Controlled Oxidative Degradation of Isotactic Polystyrene at Elevated Temperatures. II. Kinetics and Mechanism

H. H. G. Jellinek and S. N. Lipovac

*Department of Chemistry, Clarkson College of Technology, Potsdam, New York 13676.
Received May 1, 1969*

ABSTRACT: The initial stage of the oxidation process can be accounted for by diffusion control of the oxidation rate of polymer to hydroperoxide. The kinetics of the initial oxidation reaction follows quantitatively a type of Bolland mechanism. Chain scission consists of a random process due to hydroperoxide decomposition. Energies of activation have been determined for all the reactions involved in the oxidative process. The kinetics and diffusion equations for the initial stage of the oxidation are well obeyed by the experimental results. Later stages of the reaction can only be described in a qualitative or at best semiquantitative way.

Experimental results of the oxidative degradation of isotactic polystyrene were presented in part I of this paper.¹ It was pointed out there that the reaction is diffusion controlled and follows some type of Bolland mechanism. The complexity of the process becomes very large after the very initial stages, as oxygen pressure, film thickness and medium viscosity (chain scission) decrease continuously. Thus, it is only feasible to treat the very initial stages of the oxidation process quantitatively, whereas trends can only be pointed out for later stages.

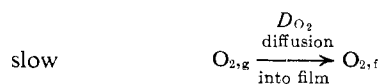
The present part of the paper deals with a quantitative evaluation of the experimental results obtained during the initial stages of the thermooxidative degradation process. It has already been pointed out that the reaction is diffusion controlled. The relevant diffusion equations are given here. Not as much use could be made of these equations as desired, since nothing is known about gas concentration gradients in the polymer at the temperatures employed here; but they give general guidelines about the reactions involved and are generally applicable under experimental conditions as encountered here.

(1) Part I: H. H. G. Jellinek and S. N. Lipovac, *Macromolecules*, **3**, 231 (1970).

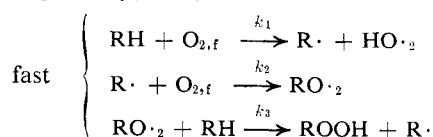
Later parts of the oxidation process are discussed only briefly due to their complexity.

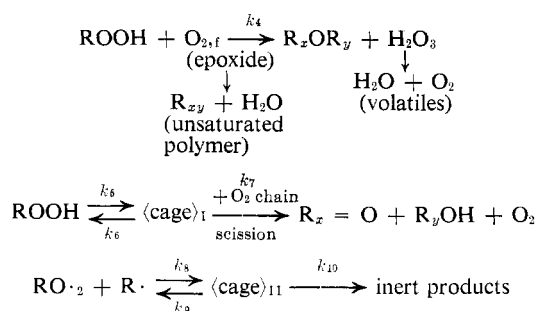
A. Initial Stages of Oxidation. Only initial stages of the oxidation process will be considered here, where the oxygen pressure and the amount of tertiary hydrogen atoms can be considered practically constant. This is a good approximation for the experiments carried out at 249 and 280°, respectively; however, it is still quite satisfactory at 300°, as only the first 6–8 min are involved. The decrease in oxygen pressure is 7% at 249°, 10% at 280°, and 25% at 300° at the end of the initial stages considered here.

A mechanism can be formulated, which accounts satisfactorily and in a quantitative way for the initial stages of the oxidation process. Here $O_{2,g}$ denotes



oxygen in the gas phase and $O_{2,f}$ oxygen in the film, respectively; D_{O_2} is the diffusion coefficient for O_2





in the film, RH, R·, RO₂·, ROO·, and ROOH stand for tertiary hydrogen atoms in the polystyrene molecule, polymer radicals, and hydroperoxide groups, respectively. Chain scission has to proceed *via* cages,² the diffusion out of cages (completed chain scission) is a rare event.

The rate of oxygen consumption in the film under steady (stationary) state conditions is given by

$$+\frac{\partial[\text{O}_2]_f}{\partial t} = D_{\text{O}_2} \frac{\partial^2[\text{O}_2]_f}{\partial x^2} - k_2[\text{O}_2]_f[\text{R} \cdot]_f = 0 \quad (1)$$

Here, x is the distance from the film surface and D_{O_2} the diffusion coefficient of O₂ in the film. From eq 1, it follows that

$$D_{\text{O}_2} \frac{\partial^2[\text{O}_2]_f}{\partial x^2} = k_2[\text{O}_2]_f[\text{R} \cdot]_f \quad (2)$$

The rate of consumption of oxygen in the gas phase is practically only due to reaction 2 of the scheme, hence (see Appendix I, eq 4')

$$-\frac{d\text{O}_{2,g}}{A dt} = -D_{\text{O}_2} \left(\frac{\partial[\text{O}_2]_f}{\partial x} \right)_{x=0} = \frac{K_{r,\text{O}_2} V_f}{A} \quad (3)$$

A is the surface area of the film and V_f is the film volume.

The reaction rate in the film is controlled by the relatively slow rate of supply of oxygen due to diffusion.

According to the mechanism (see Appendix I, eq 4')

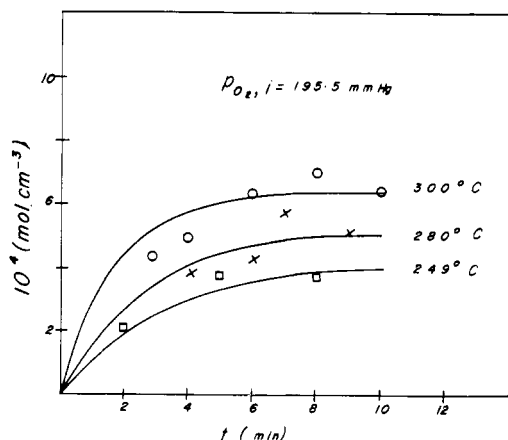


Figure 1. Calculated curves according to eq 6' and experimental points for initial stages of peroxide formation during thermooxidative degradation of isotactic polystyrene at constant initial oxygen pressure of 195.5 mm.

(2) H. H. G. Jellinek and Ming Dean Luh, *Eur. Polym. J., Suppl.*, in press.

$$\begin{aligned}
 -\frac{d\text{O}_{2,g}}{V_f dt} &= \left(\frac{d[\text{ROOH}]_f}{dt} \right)_{\text{formation only}} \\
 &= \left(\frac{k_1 k_2 k_3 (k_9 + k_{10})}{k_8 k_{10}} \right)^{1/2} [\text{RH}]_f [\text{O}_2]_f \\
 &= K_{r,\text{O}_2} = K_{\text{O}_2} [\text{O}_2]_f [\text{RH}]_f
 \end{aligned} \quad (4)$$

K_{r,O_2} is not constant in the prestationary state ($[\text{O}_2]_g \cong \text{constant}$, but $[\text{O}_2]_f \neq \text{constant}$), but rises from zero to the steady-state value with an induction period, whose length is determined by temperature and initial oxygen pressure. The steady-state K_{r,O_2} values ($[\text{O}_2]_g \cong \text{constant}$ and $[\text{O}_2]_f = \text{constant}$) were derived from the initial slopes of the plots of oxygen consumption *vs.* time. The experimental points give a slightly curved line; this means that the steady state is not completely reached; however, these slightly curved lines can be considered as straight lines, whose slopes represent good approximations to the real steady state. This implies that the $[\text{O}_2]_f$ concentration is constant with good approximation. K_{r,O_2} is proportional to the initial oxygen pressure as required by the mechanism. Experimental indications are that the straight line relationship holds at least up to 80 mm of oxygen. Calculations made on this basis give reasonable K_{r,O_2} values. Also calculations involving hydroperoxides give consistent results up to 195.5 mm on the basis of a straight line relationship according to eq 4.

The overall rate of hydroperoxide formation during the period when the oxygen concentration is near the steady state is given by (see Appendix I, eq 5')

$$\begin{aligned}
 \frac{d[\text{ROOH}]_f}{dt} &= K_{\text{O}_2} [\text{RH}]_f [\text{O}_2]_f - k_4 [\text{O}_2]_f [\text{ROOH}]_f \\
 &= K_{\text{ROOH}} - C [\text{ROOH}]_f
 \end{aligned} \quad (5)$$

where

$$K_{\text{ROOH}} = K_{r,\text{O}_2} = K_{\text{O}_2} [\text{RH}]_f [\text{O}_2]_f \quad (6a)$$

and

$$C = k_4 [\text{O}_2]_f \quad (6b)$$

Equations 6a and 6b are well obeyed. The oxygen concentration in the film is assumed to follow Henry's law. $[\text{ROOH}]_f$ (nonstationary state for hydroperoxides) is given approximately by (see Appendix I, eq 6')

$$[\text{ROOH}]_f = \frac{K_{\text{ROOH}}}{C} (1 - e^{-Ct}) \quad (7)$$

Equation 7 is also well obeyed (Figure 1, part II). The rates of hydroperoxide formation in moles/cm³ min of film are of the required magnitude (*i.e.*, almost equal to the respective rates of moles of oxygen taken up by the film).

The near stationary state for hydroperoxides coincides with the near stationary state for oxygen consumption. When the stationary states for hydroperoxide and oxygen consumption are reached, the overall rate of peroxide formation becomes zero and one obtains

$$K_{\text{ROOH}} = K_{r,\text{O}_2} = C [\text{ROOH}]_f$$

or

$$[\text{ROOH}]_f = \frac{K_{\text{ROOH}}}{C} \quad (8)$$

TABLE I
COMPARISON OF EXPERIMENTAL C VALUES AND C VALUES
CALCULATED FROM EQUATION 12

Temp, °C	$P_{O_2,i}$, mm	C , min ⁻¹ (from peroxide measure- ments)	C , min ⁻¹ (from eq 12)
300	195.5	0.54	0.53
300	97.5	0.41	0.45
300	39.0	0.22	0.23
280	195.5	0.40	0.40
249	195.5	0.30	0.27

This is the case, when the $[ROOH]_t$ concentrations reach their maximum values. The kinetic eq 7 for hydroperoxide formation requires such maximal values (see Figure 4, part I).

The overall rate of volatile formation in the film, when the steady state or near steady state is reached, is given by (see Appendix I, eq 3')

$$\frac{1}{m} \frac{d[\text{vol}]_t}{dt} = 0 = \frac{D_{\text{vol}}}{m} \frac{\partial^2 [\text{vol}]_t}{\partial x^2} + C[ROOH]_t \quad (9)$$

where m is a stoichiometric factor. Further

$$-\frac{1}{m} \frac{dM_{\text{vol},g}}{Adt} = -\frac{D_{\text{vol}}}{m} \left(\frac{\partial [\text{vol}]_t}{\partial x} \right)_{x=0} = \frac{C[ROOH]_t V_t}{A} \quad (10)$$

where A is the film surface area, $M_{\text{vol},g}$ are the moles of gas in the reaction vessel. Hence, when exactly steady-state conditions are reached, one obtains according to the proposed mechanism

$$-\frac{1}{m} \frac{dM_{\text{vol},g}}{Adt} = \frac{C[ROOH]_{f,\text{max}} V_t}{A} = \frac{K_{\text{ROOH}} V_t}{A} = \frac{1}{m} K_{\text{vol}} V_t \quad (11)$$

where K_{vol} has the dimensions of a rate cm^{-2} .

A straight line should be obtained by plotting K_{vol} vs. the initial oxygen pressure. This is actually the case. Calculated values of K_{vol} , $10^6 K_{\text{vol}}$ ($\text{mol min}^{-1} \text{cm}^{-2} [\text{mm}]^{-1}$), are 1.15, 3.13, and 6.78 at 249, 280, 300°, respectively. The following ratio is obtained from the kinetics of near steady-state conditions.

$$\frac{-\frac{1}{m} \frac{dM_{\text{vol},g}}{dt}}{[ROOH]_t V_t} = C \text{ min}^{-1} \quad (12)$$

From the mathematical derivation of the diffusion process, one obtains (see Appendix II, eq 10'' and 11'')

$$\frac{-\frac{A}{m} D_{\text{vol}} \left(\frac{d[\text{vol}]_t}{dx} \right)_{x=0}}{[ROOH]_t V_t} = C \text{ min}^{-1} \quad (13)$$

Equation 12 is well obeyed by the experimental data as is shown in Table I. Equation 13 cannot be evaluated as $D_{\text{vol}}(d[\text{vol}]_t/dx)_{x=0}$ is not known, but the latter term can be calculated when C is known.

From eq 11 it follows that

$$\frac{1}{m} K_{\text{vol}} = K_{r,O_2}/A \quad (14)$$

The following relationship also holds

$$\Delta P = P_{\text{vol}} - (P_{O_2,i} - P_{O_2,t}) = (m-1)P_{O_2,t}$$

As the volume is constant, one can also write

$$K_{\Delta P} = mK_{\text{vol}}' - K_{r,O_2}' = (m-1)K_{r,O_2}' \quad (15)$$

The m values calculated from eq 15 are 1.7, 3.0, and 3.4 at 249, 280, and 300°, respectively. Thus all experimental results are in satisfactory agreement with the proposed mechanism.

It cannot be decided with certainty whether also the volatile formation in the gas phase is diffusion controlled or not. The kinetics would be the same in either case. The energy of activation for oxygen consumption in the gas phase is 12.3 kcal/cm. This energy of activation is related to the net flux of oxygen into the film (see Appendix I, eq 1'). According to eq 4, the energy of activation should be the same for peroxide formation which was found to be 13.8 kcal/cm; this is equal to the energy of activation for oxygen uptake within experimental error (see Figure 6, part I). The oxygen flux in the film can also be written in the form (compare eq 3)

$$-\frac{dO_{2,M,g}}{Adt} = -D_{O_2} \left(\frac{\partial [O_2]_t}{\partial x} \right)_{x=0} = \frac{P_{O_2}[O_2]_{t,x=0}}{S_{O_2}l} \quad (16)$$

where $P_{O_2} = D_{O_2}S_{O_2}$ is the permeability constant, and S_{O_2} the solubility of oxygen in the film (Henry's law); l is the film thickness. Thus the energy of activation corresponds to

$$(P_{O_2}[O_2]_{t,x=0}/S_{O_2}) = D_{O_2}[O_2]_{t,x=0}$$

According to eq 11, the energy of activation for the production of volatiles in the gas phase or also for the flux of volatiles into the gas phase is given by $E_{K_{\text{ROOH}}} + E_m = 13.8 + 8.0 = 21.8 \text{ kcal/mol}$ or $E_{[ROOH]_{\text{max}}} + E_C + E_m = 7.1 + 6.9 + 8.0 = 22.0 \text{ kcal/mol}$.

These values are in satisfactory agreement with the experimentally measured energy of activation of 20.6 kcal/mol for volatile formation (see Figure 6, part I). Here again, if diffusion control takes place, $P_{\text{vol}}[\text{vol}]_{t,x=0}/S_{\text{vol}} = D_{\text{vol}}[\text{vol}]_{t,x=0}$ is related to this energy of activation. Further

$$\frac{1}{m} \frac{dM_{\text{vol},g}}{Adt} = \frac{C[ROOH]_t V_t}{A} = \frac{1}{m} \frac{P_{\text{vol}}[\text{vol}]_{t,x=0}}{S_{\text{vol}}l} \quad (17)$$

where S_{vol} is the solubility of volatiles in the film and P_{vol} the corresponding permeability constant.

The rate of random chain scission is according to the proposed mechanism given by

$$-\frac{d[n]}{dt} = k_7[\text{cage}]_t = \frac{k_7 k_5 [ROOH]_t [O_2]_t}{k_6 + k_7} \cong \frac{k_7 k_5 [ROOH]_t [O_2]_t}{k_6} \quad (18)$$

$[n]$ is the concentration of main chain links at time t . During the stationary state, which is reached after about 2–3 min, $[ROOH]_t$ remains constant (see eq 8). Hence integration of eq 18 gives $([n] \cong [n_0])$ for the degree of degradation α

$$\alpha = \frac{1}{DP_{n,t}} - \frac{1}{DP_{n,0}} = \frac{k_7 k_5 K_{\text{ROOH}} [O_2]_t}{k_6 C} t = K_{\text{exp}} t \quad (19)$$

Equation 19 is identical with the empirical equation for chain scission (see part I and Figure 7, part I). Chain scission measurements were only started after 2 min reaction time. K_{exp} was found to be directly proportional to $[\text{O}_2]_t$.

The energy of activation for K_{exp} is 17.2 kcal/mol.

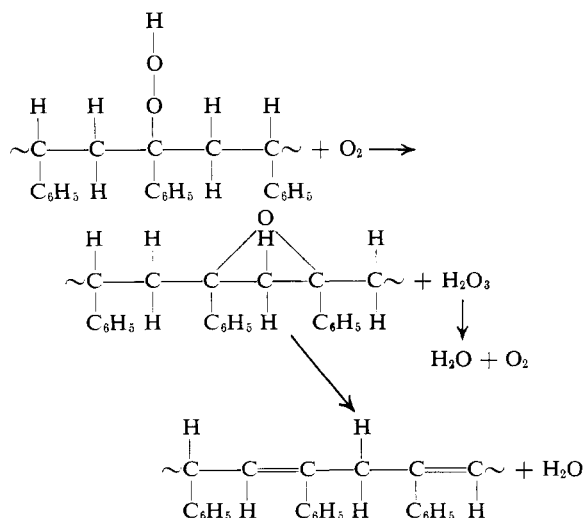
It was found that K_{ROOH} and C have energies of activation $E_{K_{\text{ROOH}}} = 7.1$ kcal/mol and $C = 6.9$ kcal/mol. Hence, for $k_7 k_5/k_6$ one has $E = 17.2 + 7.1 - 6.9 = 17.4$ kcal/mol.

It is of interest to compare the chain scission reaction results obtained for atactic polystyrene.³ First, there is a great difference in softening points of these isomers, 230° for isotactic and 83° for atactic polystyrene, respectively. The oxidation above 220° becomes very violent in the case of the atactic polymer, whereas the isotactic compound is still below its softening point. The energy of activation for chain scission for the atactic polymer is 26.2 kcal/mol, whereas the isotactic isomer gives 17.2 kcal/mol for K_{exp} . The difference may be due to increased strain in the isotactic polymer molecule. The energy of activation for actual chain rupture is not known for the mechanism, as the individual rate constants k_5 , k_6 , and k_7 cannot be determined.

It was found that, in contrast to the oxidation of isotactic polystyrene, the reaction of the atactic isomer is not diffusion controlled. In its later stages some slowing down takes place, which is assumed to be due to inhibitors formed during the reaction. The main distinguishing characteristics in the reactions of the two isomers are apparently due to the large differences in softening points. This indicates that chains of the isotactic polymer are stiffer than those in the atactic polymer. The C-C bonds seem to be weaker in the isotactic compound than in the atactic one, due to strain.

The initial changes in ultraviolet absorbances at λ 245 m μ give an energy of activation of 23.1 kcal/mol, which is a value near that for volatile formation. The increase in absorbance seems to be due to double bond and carbonyl formation (see Figure 9, part I).

Chromatography data indicate that the main product of oxidation during the initial stages is water. This could be formed by the following tentative reactions.



(3) H. H. G. Jellinek, *J. Polym. Sci.*, **4**, 1 (1949).

H_2O_3 is a fairly stable compound, its half-life is about 2 sec.⁴ The above scheme would account for the increase in uv absorption and for the formation of more than 1 mol of water for each mole of hydroperoxide decomposed.

B. Later Stages of the Oxidation Process. It was pointed out above that the oxygen pressure, the thickness of the film and the medium viscosity will decrease continuously during the later stages of the process. Also the amount of tertiary hydrogen atoms will be depleted and the number of main chain links will not remain constant. In addition, several kinds of secondary reactions will become more dominant. Thus, it would seem that a quantitative account of these stages is not feasible at present. The experimental curves (see Figures 12 and 13, part I) show slowing down after the initial stages and eventually become approximately straight lines. The energy of activation derived from the straight lines of the later stage of oxidation gives an average energy of activation of 16.2 kcal/mol for a pressure range of 90–200 mm. The overall peroxide formation does not remain on a plateau as required by eq 7, but decreases and eventually increases again. At 249° the decrease is most pronounced (see Figures 12 and 13, part I), whereas at higher temperatures a smaller dip occurs after which the peroxide concentration increases again.

A number of experiments were carried out with purified polymer, but leaving the 20% of atactic polymer in the sample. A typical curve of pressure increase is shown in Figure 11, part I. It appears that the atactic component reacts faster than the isotactic one and is eliminated first.

The chromatograms (see Figure 14a and b, part I) give the composition of the residues of isotactic and atactic polystyrene, respectively, after prolonged thermal oxidation at 300° at an oxygen pressure of 300 mm in a closed system. The initial amounts of either polymer were similar. The data show the presence of the same compounds in the residue of either polymer. The products are much more numerous at 300° than at 249°. The one difference in composition is due to an unidentified compound D only present in the residue of the atactic polymer. The relative amounts of components A, B and monomer are larger in the residue of the isotactic than atactic polymer. Benzoic acid is present in greater amount in the residue of the atactic than in the isotactic polymer. It has been found⁵ that the stereoregularity of polystyrene affects the nature of products even when degradation is carried out at 360°.

Acknowledgment. The authors are indebted to Dr. F. C. Goodrich of the Chemistry Department, Clarkson College, for the derivation of the diffusion equations (Appendix II). They also wish to thank the U. S. Army Office of Research, Durham, N. C., for a Grant (No. DA-ARO-D-31-124-G984), which made this work possible.

(4) G. Czapski and B. H. J. Bielski, *J. Phys. Chem.*, **67**, 2180 (1963).

(5) N. A. Magrupoc, N. A. Slovohotova, S. G. Vinogradova, and V. A. Kargin, *Vysokomol. Soedin.*, **9B**, 277 (1967).

Appendix

I. Kinetics (for initial stages only, oxygen pressure = constant and $[RH] = \text{constant}$)

steady state (or near steady state)

$$k_1[RH]_t[O_2]_t = k_8[RO \cdot]_t[R \cdot]_t - k_9[\langle \text{cage} \rangle]_t \quad (1')$$

$$[\langle \text{cage} \rangle]_t = \frac{k_8[RO \cdot]_t[R \cdot]_t}{k_9 + k_{10}}$$

Further

$$[RO \cdot]_t[R \cdot]_t = \frac{k_1(k_9 + k_{10})[RH]_t[O_2]_t}{k_8 k_{10}}$$

Hence

$$[RO \cdot]_t \cong \frac{k_2[R \cdot]_t[O_2]_t}{k_3[RH]_t}$$

or

$$[RO \cdot]_t = \left\{ \frac{k_1 k_2 (k_9 + k_{10})}{k_3 k_8 k_{10}} \right\}^{1/2} [O_2]_t \quad (2')$$

and

$$[R \cdot]_t = \left\{ \frac{k_1 k_3 (k_9 + k_{10})}{k_2 k_8 k_{10}} \right\}^{1/2} [RH]_t \quad (3')$$

Oxygen consumption is practically only given by reaction 2' of the scheme, hence

$$-\frac{d[O_2]_t}{dt} = k_2[R \cdot]_t[O_2]_t = K_{O_2}[RH]_t[O_2]_t = K_{r,O_2} \quad (4')$$

where

$$K_{O_2} = \left\{ \frac{k_1 k_2 k_3 (k_9 + k_{10})}{k_8 k_{10}} \right\}^{1/2}$$

K_{r,O_2} is a linear function of the oxygen pressure.

The formation of hydroperoxides is given by the following equations (chain scission is only a minor side reaction in this connection)

$$\begin{aligned} \frac{d[ROOH]_t}{dt} &= k_3[RO \cdot]_t[RH]_t - k_4[O_2]_t[ROOH]_t \\ &= K_{O_2}[O_2]_t[RH]_t - k_4[O_2]_t[ROOH]_t \quad (5') \\ &= K_{ROOH} - C[ROOH]_t \end{aligned}$$

where $K_{ROOH} = K_{r,O_2}$ and $C = k_4[O_2]_t$. The latter two constants are both linear functions of the oxygen pressure (Henry's law); this is borne out by experiment.

Integration of eq 5' gives (this is an approximation as $[O_2]_t$ is not constant until the stationary state is reached, but for the major part of the reaction $[O_2]_t$ is fairly near the steady state concentration)

$$[ROOH]_t = \frac{K_{ROOH}}{C} (1 - e^{-Ct}) \quad (6')$$

Equation 6' is quite well obeyed by the experimental results (see Figure 1). When the exact steady state is reached, one has

$$\frac{d[ROOH]_t}{dt} = 0 = K_{ROOH} - C[ROOH]_t \quad (7')$$

Thus, $[ROOH]_t$ is constant and has reached its maximum value.

Volatile formation is given by the decomposition of hydroperoxides. For the near steady state one obtains

$$\begin{aligned} \frac{d[\text{vol}]_t}{dt} &= mC[ROOH]_t \\ &= mK_{ROOH}(1 - e^{-Ct}) \quad (8') \end{aligned}$$

Ct has rather large values after a few minutes and can be neglected, hence integration of eq 8' gives

$$[\text{vol}]_t = mK_{ROOH}t = mK_{r,O_2}t \quad (9')$$

The concentration of volatiles is a linear function of $[O_2]_t = K'P_{O_2,i}$ (Henry's law). This is actually the case. When steady state is exactly reached, one has

$$[\text{vol}]_t = mC[ROOH]_{\text{max}}t$$

where $t \geq t_{\text{max}}$.

II. Diffusion. The equation for oxygen uptake and the oxidation of the polymer (hydroperoxide) is at steady state

$$D_{O_2} \frac{\partial^2 [O_2]_t}{\partial x^2} - K_{r,O_2} = 0 \quad (1'')$$

one has also

$$K_{r,O_2} - K_{ROOH} = 0 \quad (2'')$$

Here D_{O_2} is the diffusion coefficient for oxygen in the film and x is the distance from the surface of the film.

Further, the formation of volatiles is given by the decomposition of hydroperoxides, and their diffusion out of the film,

$$D_{\text{vol}} \frac{\partial^2 [\text{vol}]_t}{\partial x^2} + mC[ROOH]_t = 0 \quad (3'')$$

The boundary conditions are $m d[O_2]_t/dx = d[\text{vol}]_t/dx = 0$ at $x = l$ where l is the film thickness. $[O_2]_t = K'[O_2]_g$ (Henry's law) at $x = 0$ and $[\text{vol}]_t = 0$ at $x = 0$.

Solutions

$$[O_2]_t = K'[O_2]_g \frac{\cosh \sqrt{\frac{K_{O_2}}{D_{O_2}}}(l-x)}{\cosh \sqrt{\frac{K_{O_2}}{D_{O_2}}}l} \quad (4'')$$

$$[\text{vol}]_t = mK'[O_2]_g \frac{D_{O_2}}{D_{\text{vol}}} \left[1 - \frac{\cosh \sqrt{\frac{K_{O_2}}{D_{O_2}}}(l-x)}{\cosh \sqrt{\frac{K_{O_2}}{D_{O_2}}}l} \right] \quad (5'')$$

$$[ROOH]_t = K'[O_2]_g \frac{K_{O_2} \cosh \sqrt{\frac{K_{O_2}}{D_{O_2}}}(l-x)}{C \cosh \sqrt{\frac{K_{O_2}}{D_{O_2}}}l} \quad (6'')$$

The flux of oxygen into the film and the exit flux of volatiles are given by

$$D_{O_2} \left(\frac{d[O_2]_f}{dx} \right) = \frac{l}{m} D_{vol} \left(\frac{d[vol]_f}{dt} \right)_{x=0} = \left[\tanh \left(\frac{K_{O_2} l^2}{D_{O_2}} \right)^{1/2} \right] \text{mol cm}^{-2} \quad (9'')$$

$$K'[O_2]_g \sqrt{K_{O_2} D_{O_2}} \tanh \sqrt{\frac{K_{O_2}}{D_{O_2}}} l \text{ mol cm}^{-2} \text{ sec}^{-1} \quad (7'')$$

The total peroxide amount in the film is

$$\int_0^l [ROOH]_f dx = K'[O_2]_g \frac{\sqrt{K_{O_2} D_{O_2}}}{C} \tanh \sqrt{\frac{K_{O_2}}{D_{O_2}}} l \text{ mol cm}^{-2} \quad (8'')$$

and the total volatiles in the film

$$\int_0^l [vol]_f dx = mK'[O_2]_g \frac{D_{O_2} l}{D_{vol}} \left[1 - \left(\frac{D_{O_2}}{K_{O_2} l^2} \right)^{1/2} \times \right.$$

If l is large, the following approximations hold

flux of volatiles =

$$mK'[O_2]_g \sqrt{K_{O_2} D_{O_2}} \text{ mol cm}^{-2} \text{ sec}^{-1} \quad (10'')$$

$$\text{total peroxide in film} = K'[O_2]_g \frac{\sqrt{K_{O_2} D_{O_2}}}{C} \text{ mol cm}^{-2}$$

(11'')

$$\text{total volatiles in film} = mK'[O_2]_g \frac{D_{O_2} l}{D_{vol}} \text{ mol cm}^{-2}$$

(12'')

The Glass Temperature of Linear Polyethylene¹

Ferdinand C. Stehling and

Plastics Research Laboratory, Esso Research and Engineering Co., Baytown, Texas 77520

Leo Mandelkern

Department of Chemistry and Institute of Molecular Biophysics, Florida State University, Tallahassee, Florida 32306. Received December 4, 1969

ABSTRACT: Transitions in linear polyethylene (LPE) samples encompassing a wide range of fractional crystallinity, 0.46–0.85, have been examined with the objective of ascertaining the glass transition temperature, T_g , of this polymer. Thermal expansion, calorimetric, and dynamic mechanical measurements lead to the conclusion that the γ transition at *ca.* -130° is the primary glass transition of LPE. At temperatures below the γ transition, the coefficient of thermal expansion, α , is almost independent of crystallinity, whereas at temperatures slightly above this transition, α increases systematically as the degree of crystallinity decreases. The quantitative behavior of α above and below the γ transition in LPE is very similar to that of other crystalline polymers at their respective glass temperatures. Furthermore, the value of α estimated for completely amorphous LPE below the γ transition is similar to that of completely amorphous polymers below T_g ; and the value of α estimated for completely amorphous LPE slightly above the γ transition is similar to that of wholly amorphous polymers above T_g . Qualitative calorimetric measurements show that the heat capacity of LPE with low levels of crystallinity increases across the γ transition. The magnitude and character of the heat capacity change in the γ region for the least crystalline LPE sample is similar to that of semicrystalline polydimethylsiloxane at the T_g , -123° , of this polymer. Dynamic mechanical measurements show that the intensity of the γ relaxation increases as crystallinity decreases. The observed asymmetry of the γ relaxation is interpreted in terms of two overlapping relaxations arising from the noncrystalline domains of the polymer. A simple morphological model is suggested which satisfactorily accounts for the results of a large number of wide-line nmr and dynamic mechanical experiments made on melt and solution crystallized LPE. Since other investigators have proposed that the T_g of polyethylene is *ca.* -80° or *ca.* -20° , these temperature regions were also closely examined. However, even in the LPE samples with low levels of crystallinity, transitions in these temperature regions were, at most, barely detectible. Transitions in these temperature ranges, if they exist at all, do not have the typical characteristics of a primary glass transition.

The relaxations of linear and branched polyethylene have been extensively examined by numerous investigators, and the experimental results have been reviewed by Boyer,² McCrum, Read, and Williams,³ and by McKenna, Kajiyama, and MacKnight.⁴ Dynamic mechanical measurements made at low frequencies on branched polyethylene show loss maxima at

ca. $+70$, -20 , and -120° that have been termed the α , β , and γ relaxations, respectively. The α and γ relaxations have also been observed in all dynamic mechanical studies of linear polyethylene (LPE), but the β relaxation in LPE has been found to be either absent^{5–7} or barely detectible.^{8–11} Most investigators,

(5) V. L. Bohn, *Kolloid Z.*, **194**, 10 (1964).

(6) R. K. Eby and J. P. Colson, *J. Acoust. Soc. Amer.*, **39**, 505 (1966).

(7) K. M. Sinnott, *J. Appl. Phys.*, **37**, 3385 (1966).

(8) R. S. Moore and S. Matsuoka, *J. Polym. Sci., Part C*, **5**, 163 (1964).

(9) W. Pechhold, V. Eisele, and G. Knauss, *Kolloid Z.*, **196**, 27 (1964).

(10) V. K. H. Illers, *Rheol. Acta*, **3**, 202 (1964).

(11) D. E. Kline, J. A. Sauer, and A. E. Woodward, *J. Polym. Sci.*, **22**, 455 (1956).

(1) This work was supported in part by a grant from the Army Research Office (Durham).

(2) R. F. Boyer, *Rubber Chem. Technol.*, **36**, 1303 (1963).

(3) N. G. McCrum, B. E. Read, and G. Williams, "Anelastic and Dielectric Effects in Polymeric Solids," John Wiley & Sons, Inc., New York, N. Y., 1965, p 353 ff.

(4) L. W. McKenna, T. Kajiyama, and W. J. MacKnight, *Macromolecules*, **2**, 58 (1969).